Jyväskylän yliopiston julkaisuarkisto
Jyväskylä University Digital Archive

UNIVERSITY OF JYVÄSKYLÄ

This is an electronic reprint of the original article.
This reprint *may differ* from the original in pagination and typographic detail.

Author(s): Airaksinen, Tuomas; Mönkölä, Sanna

Title: Comparison between the shifted-Laplacian preconditioning and the controllability methods for computational acoustics

Year: 2010

Version:

Please cite the original version:

Airaksinen, T., & Mönkölä, S. (2010). Comparison between the shifted-Laplacian preconditioning and the controllability methods for computational acoustics. Journal of Computational and Applied Mathematics, 234(6), 1796-1802. https://doi.org/10.1016/j.cam.2009.08.030

All material supplied via JYX is protected by copyright and other intellectual property rights, and duplication or sale of all or part of any of the repository collections is not permitted, except that material may be duplicated by you for your research use or educational purposes in electronic or print form. You must obtain permission for any other use. Electronic or print copies may not be offered, whether for sale or otherwise to anyone who is not an authorised user.

Comparison between the shifted-Laplacian preconditioning and the controllability methods for computational acoustics

Tuomas Airaksinen [a,*] Sanna Mönkölä [a]

[a] *Department of Mathematical Information Technology, University of Jyväskylä, P.O. Box 35 (Agora), FI-40014 University of Jyväskylä, Finland*

Abstract

Processes that can be modeled with numerical calculations of acoustic pressure fields include medical and industrial ultrasound, echo sounding, and environmental noise. We present two methods for making these calculations based on Helmoltz equation. The first method is based directly on the complex-valued Helmholtz equation and an algebraic multigrid approximation of the discretized shifted-Laplacian operator; i.e. the damped Helmholtz operator as a preconditioner. The second approach returns to a transient wave equation, and finds the time-periodic solution using a controllability technique. We concentrate on acoustic problems, but our methods can be used for other types of Helmholtz problems as well. Numerical experiments show that the control method takes more CPU time, whereas the shifted-Laplacian method has larger memory requirement.

Key words: Helmholtz equation, computational acoustics, algebraic multigrid method, preconditioner, exact controllability, finite element method, spectral element method
MSC: 93B05, 35J05, 65N30, 65N35

1 Introduction

The many applications of computational acoustics in industry range from medical measurement to machinery design. Computational acoustics enables the simulation of situations that would be difficult to explore experimentally.

* Corresponding author.
Email address: tuomas.airaksinen@jyu.fi (Tuomas Airaksinen).

Article published in Journal of Computational and Applied Mathematics 234 (2010) 1796–1802

Compared to experiments, computer simulations provide a safe, fast, and cost-efficient way of providing guidelines for acoustical applications. Nevertheless, solving problems arising from real life acoustic applications by computer demands a considerable amount of time and memory. In particular, high frequency phenomena are computationally demanding. This is because the resolution of the spatial discretization needs to be adjusted to the frequency to achieve accurate results. Furthermore, solutions with high frequency suffer from numerical dispersion. This so-called pollution effect [1] cannot be avoided in two- and three-dimensional problems [2], but it can be reduced by using higher order polynomial basis [3,4], among other methods. However, the pollution error in discretizations necessitates finer meshes for high-frequency problems.

Our aim is to develop efficient iterative solution methods for acoustic problems, which are modelled by the Helmholtz equation presented in Section 2. Element methods, such as the finite element method (FEM) and the spectral element method (SEM), have emerged as generic tools for discretizing the Helmholtz equation. The review [5] describes research efforts on this field (see also [6,7]). Finite element discretizations of the Helmholtz equation are non-Hermitian and indefinite. For mid-frequency and high-frequency problems, the resultant matrix can be extremely large, which often limits the feasible size of the scattering problem under consideration. As a result, the finite element discretizations of the Helmoltz equation are a challenge for the current solvers, and require the use of iterative methods such as the GMRES method or the BICGSTAB method [8]. These methods, in turn, require a good preconditioner for the discretized Helmholtz equations in order to have reasonably fast convergence.

In Section 3, we consider a shifted-Laplacian preconditioner that is obtained from the discretized damped Helmholtz operator. A preconditioner based on approximating a damped Helmholtz operator by a geometric multigrid cycle was considered in [9]. There, the scattering problems were posed on a rectangular domain and they were discretized using low-order finite differences, and a geometric multigrid method was used. Quadratic and cubic finite elements in particular helped to reduce the number of unknowns in order to reach prescribed accuracy, as they have much smaller interpolation and pollution errors than linear basis functions [1]. The preconditioner used in this paper, employs an algebraic multigrid (AMG) method in the approximation of the damped Helmholtz operator. In particular, the preconditioner can be constructed purely algebraically when the matrix for the 0^{th} order terms is also available.

An alternative iterative approach suitable for solving the Helmholtz equation via the time-dependent wave-equation is presented in Section 4. The basic idea is to find a time-periodic solution to wave equations by using a controllability

method. This leads to preconditioned conjugate gradient iterations for initial data. This technique was introduced for the Helmholtz equation by Bristeau, Glowinski, and Périaux [10,11]. They used low order finite elements for space discretization and second order central finite differences for time discretization. Since low order discretizations lead to poor accuracy, we have made improvements to the method. In [12], we used higher order spectral elements for space discretization. We noticed that second order time discretization limits the accuracy with elements of order $r = 3$ or higher, unless very fine time steps are used. That is why the fourth order Runge-Kutta time discretization was applied to the method in [13]. Higher order discretizations in both space and time domain provide high accuracy. However, with higher order discretizations the computational cost is larger than with lower order discretizations.

Comparison between the shifted-Laplacian and the controllability methods is presented in Section 5 with respect to CPU time and memory usage. Although the computational grids are not the same for both methods, the same number of discretization points is used for both methods to make comparisons reasonable. The accuracy of the discretizations is compared as well.

The methods that we use are not restricted to a certain application but can be suited to simulate several real life problems. Hence, our examples do not focus on a specific application. However, geometrical shapes similar to those used in our scattering examples can be used in several applications in audio technology and echo sounding. For example, noise barriers with cross sections as presented in our scattering examples can be used in environmental noise attenuation. In this setting, simulation results show where the noise is reduced to a certain level. In echo sounding, one can determine the location of the highest echo signal.

2 The Helmholtz equation and boundary conditions

Acoustic scattering can be described by the Helmholtz equation

$$-\nabla \cdot \frac{1}{\rho(\mathbf{x})} \nabla u - \frac{k(\mathbf{x})^2}{\rho(\mathbf{x})} u = 0, \tag{1}$$

where u denotes the complex-valued time-harmonic acoustic pressure field, $k(\mathbf{x}) = \omega / c(\mathbf{x})$ is the wave number, $\rho(\mathbf{x})$ is the density of the material, ω is the angular frequency of the sound, $c(\mathbf{x})$ is the speed of sound, and $\mathbf{x} = (x_1, x_2) \in \mathbb{R}^2$ is the space variable. The wave number k varies depending on location as materials change.

We consider two different boundary conditions: the Dirichlet boundary con-

dition and the absorbing boundary condition. We decompose the boundary $\Gamma = \partial\Omega$ into two parts, Γ_d and Γ_a such that $\Gamma = \Gamma_d \cup \Gamma_a$. The Dirichlet boundary Γ_d is sound-soft and is described by the Dirichlet boundary condition

$$u = g_d \quad \text{on } \Gamma_d, \tag{2}$$

where function g_d gives the sound source.

The absorbing boundary condition should let outgoing waves propagate out of the domain without reflections, as the Sommerfeld radiation condition requires. Considering a perfect absorbing boundary condition as a non-local operator is computationally difficult, but it can be approximated by a local operator [14]. We use here the absorbing boundary condition

$$-ik(\mathbf{x})u + \frac{\partial u}{\partial \mathbf{n}} = g_a \quad \text{on } \Gamma_a, \tag{3}$$

with the imaginary unit $i = \sqrt{-1}$, outer normal vector $\mathbf{n}$, and source term g_a.

3 The Finite element method and preconditioning with the shifted-Laplacian

In the finite element method, the weak formulation of the Helmholtz equation is used to form the discretized version of the equation. The weak form and corresponding spaces that are used here are identical to the ones described in [15]. The finite element discretization is made on a triangulation given by a set of non-overlapping triangles K_h such that $\Omega_h = \bigcup_{\tau \in K_h} \tau$. Here h corresponds to the largest distance between discretization nodes and Ω_h is an approximation of the computational domain Ω. In this paper, linear and cubic finite elements are employed. They correspond to the first and third order Lagrangian polynomials as basis functions of elements, respectively. Ultimately, a system of linear equations

$$\mathbf{A}\mathbf{u} = \mathbf{f}, \tag{4}$$

is obtained, where $\mathbf{A}$ is a sparse matrix, $\mathbf{u}$ is the vector that contains the values of u on triangulation nodes and $\mathbf{f}$ is a non-zero vector arising from the sound source.

In this case, $\mathbf{A}$ is indefinite and symmetric but non-Hermitian. Hence, the generalized minimal residual (GMRES) method [8] is a suitable iterative method for the sparse matrix equation (4). In the numerical experiments we use the full GMRES method without restarts.

Except for very small-scale problems, the system (4) is generally badly conditioned, and it leads to very slow convergence of Krylov subspace methods when

applied directly to the system (4). To improve the conditioning and the speed of convergence, we right-precondition (4) by $\mathbf{B}^{-1}$ and solve the preconditioned system

$$\mathbf{A}\mathbf{B}^{-1}\tilde{\mathbf{u}} = \mathbf{f}, \quad \mathbf{u} = \mathbf{B}^{-1}\tilde{\mathbf{u}}. \tag{5}$$

The goal is to find a preconditioner $\mathbf{B}$ such that the matrix $\mathbf{A}\mathbf{B}^{-1}$ is well conditioned and multiplication of vectors by $\mathbf{B}^{-1}$, i.e. solving systems with the matrix $\mathbf{B}$, can be done with a small computational effort. These ideal properties would lead to a fast convergence of the iterative method at a small overall computational cost.

In this paper, the preconditioner is based on a discretized form of the shifted-Laplacian operator $\mathcal{B}_{SL} = -\nabla \cdot \frac{1}{\rho(\mathbf{x})}\nabla - (\beta_1 + \beta_2 i)\,\frac{k(\mathbf{x})^2}{\rho(\mathbf{x})}$, as originally presented in [16]. By choosing $\beta_1 = 1$ and β_2 to be positive, $\mathcal{B}_{SL}$ corresponds to damped Helmholtz operator. In [15], the algebraic multigrid method (AMG) was used to approximate inversion of $\mathcal{B}_{SL}$. We use this preconditioner here and denote it by $\mathbf{B}_{MG}$. When evaluating $\mathbf{B}_{MG}^{-1}$ with the AMG method, we use one W-cycle with underrelaxed Jacobi method with relaxation parameter $\omega_{\text{jac}} = 0.4$ as the smoothener. One iteration of the Jacobi is used as a pre- and post-smoothener. The damping parameter β_2 is chosen to be 0.5, which was found to be a good choice in [15].

4 A control based approach with spectral elements

An alternative approach to solving the Helmholtz equation is based on finding a time-periodic solution of the associated transient wave equation via an exact controllability technique. To obtain the time-harmonic solution, we minimize the difference between initial conditions and the corresponding variables after one time period $T = 2\pi/\omega$. Proceeding this way, the problem of time-harmonic wave scattering can then be cast as a least squares problem

$$\min \left(\frac{1}{2}\int_\Omega \left| \frac{\partial U(T)}{\partial t} - e_1 \right|^2 dx + \frac{1}{2}\int_\Omega \left| \nabla (U(T) - e_0) \right|^2 dx \right), \tag{6}$$

where the initial conditions are contained in a vector $(e_0, e_1)^T = (U(0), \frac{\partial U}{\partial t}(0))^T$, and $U(t) = \mathrm{Re}(e^{-ikt}u)$ satisfies the time-dependent equations associated with the system (1)-(3).

The time-dependent wave equation and the function to be minimized in (6) are discretized in space domain with the spectral element method [3]. We use higher-order Lagrange interpolation polynomials as basis functions, and the nodes of these functions are placed at the Gauss-Lobatto discretization points. The integrals in the weak form of the equation are evaluated with

the corresponding Gauss-Lobatto quadrature formulas. This leads to semi-discretized state equation

$$\mathbf{M}\frac{\partial^2 \mathbf{U}}{\partial t^2} + \mathbf{S}\frac{\partial \mathbf{U}}{\partial t} + \mathbf{K}\mathbf{U} = \mathbf{F}, \tag{7}$$

where $\mathbf{U}$ is the global vector containing the values of the pressure $U(t)$ at the Gauss-Lobatto points of the quadrilateral mesh, $\mathbf{M}$ is the mass matrix, $\mathbf{S}$ is the matrix arising from the absorbing boundary condition, $\mathbf{K}$ is the stiffness matrix, and $\mathbf{F}$ is the vector due to the source functions $\mathrm{Re}\left(e^{-ikt}g_d\right)$ and $\mathrm{Re}\left(e^{-ikt}g_a\right)$. The least squares problem, where the function to be minimized is semi-discrete form, is

$$\min\left(\frac{1}{2}\left(\mathbf{U}(T)-e_0\right)^T\mathbf{K}\left(\mathbf{U}(T)-e_0\right)+\frac{1}{2}\left(\frac{\partial \mathbf{U}(T)}{\partial t}-e_1\right)^T\mathbf{M}\left(\frac{\partial \mathbf{U}(T)}{\partial t}-e_1\right)\right).$$

For time discretization we use the fourth order Runge-Kutta method.

The discretized minimization problem is solved by a preconditioned conjugate gradient (CG) algorithm. We use a block-diagonal preconditioner $\mathrm{diag}\,(\mathbf{K},\mathbf{M})$. The linear systems with the stiffness matrix $\mathbf{K}$ are solved by the algebraic multigrid method [17,15,13]. As a smoother for the AMG, we apply the successive over relaxation (SOR) method with relaxation factor equal to 1.2. One iteration of the SOR is used for a pre- and post-smoothener. Additionally, at the beginning of every multigrid iteration, four iterations of the SOR are used to smooth the solution initially. The so-called W-cycle [18] is utilized as a multigrid iteration until the residual norm of the solution is smaller than 10^{-6}.

5 Numerical experiments

We compared the efficiency of the methods, presented in Sections 3 and 4, by performing tests considering accuracy, computational cost and memory requirement. In both methods, the overall accuracy of the discrete solution depends on spatial discretization (performed by higher order element methods with mesh step size h and element order r), the stopping criterion ε of the iterative method (GMRES or CG), approximation of the geometrical boundaries, and approximation of the radiation condition.

In the shifted-Laplacian method, we used an unstructured triangular mesh generated with Comsol Multiphysics 3.3. For the control method, a mesh consisting of polygonal elements was created by a mesh generator from Numerola Ltd. The meshes are built such that approximate number of discretization

points is same for both methods. Since good efficiency can be achieved with higher order elements by using sufficiently large mesh step size, we have used constant spatial discretization between different element orders (i.e., r/h is constant).

In [15,12,13], it is shown that the number of iterations needed to achieve a given stopping criterion is independent of the element order. Since with lower order elements we can save CPU time by using rougher stopping criterion without loss of accuracy, we have used stopping criterion $\varepsilon = 10^{-(r+2)}$ with both methods for element order r, unless otherwise mentioned. In accuracy tests, we have used polygonal boundaries to avoid the error from approximating the geometry, in connection with a test problem that satisfies the absorbing boundary condition. Errors between the real parts of the analytical solution and the computational result are reported as L^∞-norms.

Time discretization, performed by the fourth order Runge-Kutta scheme, affects the accuracy of the control method. To eliminate the temporal error, for elements of order r we use a timestep of length $\Delta t = \alpha_r h_{min}/c_{max}$, where $\alpha_1 = 2/3, \alpha_2 = 1/5, \alpha_3 = 7/80$, and $\alpha_4 = 5/90$. Here, h_{min} denotes the minimum mesh step size and c_{max} denotes the maximum sound speed.

Throughout the tests, we have chosen to use the propagation direction $(-1, 1)$, which is determined by wave vector $\mathbf{k} = \frac{1}{\sqrt{2}}(-1, 1)\, k$. The starting values $(e_0, e_1)^T$ for the control method are set by the procedure presented in [13]. All computations have been carried out on an AMD Opteron 885 processor at 2.6 GHz. In the figures and tables, we use the abbreviation *SL method* for the shifted-Laplacian method.

5.1 Accuracy

The domain Ω, consisting of a fluid with density $\rho = 1$, is defined so that its outer boundary, Γ_a, coincides with the boundary of the rectangle $[0, 4] \times [0, 4]$. We have set a square obstacle, having a side length of 2 and boundary Γ_d in

Table 1
Number of nodes and number of space discretization points for different element orders in the coarsest meshes.

	SL method		Control method			
Element order	1	3	1	2	3	4
Mesh step size h	0.025–0.084	0.097–0.252	0.050	0.100	0.143	0.200
Number of nodes in mesh	5075	610	5040	1320	672	360
Number of space discretization points	5075	5142	5040	5040	5544	5040

the center of the domain Ω. The error arising from the approximation of the absorbing boundary condition is eliminated by solving the Helmholtz problem with $g_d = e^{i\mathbf{k}\cdot\mathbf{x}}$ and $g_a = i\,(k_1 n_1 + k_2 n_2 - k)\, e^{i\mathbf{k}\cdot\mathbf{x}}$. The function $u = e^{i\mathbf{k}\cdot\mathbf{x}}$ satisfies this problem, and the solution of the corresponding time-dependent equation is $U = \cos(kt - \mathbf{k}\cdot\mathbf{x})$. The accuracy of the methods is compared with a series of tests where mesh step size is halved consecutively, starting from the meshes introduced in Table 1.

In the first accuracy experiment, we used angular frequency $\omega = 2\pi$ and wave speed $c(\mathbf{x}) = 1$ corresponding to the constant wave number $k = 2\pi$. As mesh refinement with a constant wave number leads to more accurate results, we also refine the stopping criterion in this particular test, as opposed to the usual stopping criterion $\varepsilon = 10^{-(r+2)}$ for r^{th}-order elements. Theoretically, the asymptotic maximum error between the analytical solution and the computed solution is divided by four for the element order $r = 1$ and by sixteen for $r = 3$, when the total number of elements in the mesh is multiplied by four (i.e., the mesh step size is divided by two). To guarantee that the stopping criterion does not limit the accuracy, we have used stopping criteria $\varepsilon = 10^{-3}, 5{\cdot}10^{-4}, 10^{-4}, 5{\cdot}10^{-5}, 10^{-5}$ for $r = 1$ with increasing mesh density. Respectively, within each mesh refinement for $r = 3$, we have divided the stopping criterion by ten. The results with element orders $r = 1$ and $r = 3$, plotted in Figure 1, are in line with the theoretical consideration, and they show that using higher order elements is better then refining the mesh when high efficiency is needed. With the control method in particular, the computations with fine grids are inefficient since small time steps need to be used to satisfy the stability and accuracy demands. Consequently, to obtain the prescribed level of the the residual for the three smallest values of h and Δt with spectral elements and $r = 3$, more than 1000 iterations (our maximum number of iterations) are required.

Because solving acoustic problems with large frequencies is of special interest, we have performed another set of experiments by doubling the angular frequency with every mesh refinement. In these tests, we have set ωh constant for angular frequencies $\omega = 2\pi, 4\pi, 8\pi, 16\pi, 32\pi$, and the number of space discretization points has been approximately 20 per wavelength. The results presented in Figure 2 for the shifted-Laplacian method with $r = 1, 3$ and the control method with $r = 1, 2, 3, 4$ show how the pollution error deteriorates the accuracy as the frequency becomes larger. The lowest order elements ($r = 1$) become useless with both methods as the angular frequency increases. The higher-order methods appear to be the most effective in both respects. We see that better accuracy is gained by the control method with spectral element discretization, but the shifted-Laplacian method with triangular finite elements appears to be faster. Due to the comparatively large discretization error in connection with our triangular space discretization, the pollution error is not clearly visible for the cubic elements ($r = 3$) within the frequency range

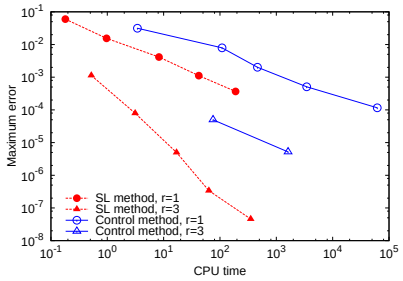

Figure 1. Errors with respect to CPU time (in seconds). On each line, mesh step size is divided by two, consecutively, and angular frequency $\omega = 2\pi$ is kept constant.

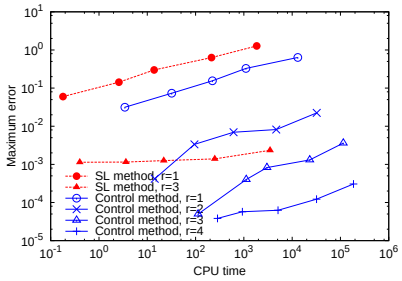

Figure 2. Errors with respect to CPU time (in seconds). On each line, there are points for angular frequencies $\omega = 2\pi, 4\pi, 8\pi, 16\pi, 32\pi$ when ωh is a constant giving approximately 20 discretization points per wavelength.

used in this experiment. However, it is possible to improve the accuracy at the expense of computational time with triangular elements by using denser discretization mesh.

5.2 Scattering

We illustrate acoustic scattering by solving the Helmholtz problem with $g_d = 0$ and $g_a = i\,(k_1 n_1 + k_2 n_2 - k)\,e^{i\mathbf{k}\cdot\mathbf{x}}$ in both homogeneous and heterogeneous domains. The outer boundary of the domain coincides with the boundary of the rectangle $[-3/4, 3/4]\times[-3/4, 3/4]$. Density is assumed to be constant $\rho(\mathbf{x}) = 1$. For tests in homogeneous domain we have used $c(\mathbf{x}) = 1$. In the heterogeneous test case, parameters are the same, except $c(\mathbf{x}) = 1.5$ for $x_1 \notin [-3/20, 3/20]$. Our methods can be applied to complex geometries as well, and as an example of such a geometry we have chosen a crescent-shaped scatterer. The scatterer can be described as the set of points inside the closed disk of radius $3\sqrt{2}/20$ centered at the origin but outside the open disk of radius $3\sqrt{2}/20$ centered at $(3/10, 0)$. See Figure 4.

In these tests, we have used angular frequencies $\omega = 12\pi, 24\pi, 48\pi, 96\pi, 192\pi$ for element orders $r = 1, 3$. The scattering problems are solved by using constant ωh, implying approximately 10 space discretization points per wave length in the homogeneous domain and for $x_1 \in [-3/20, 3/20]$ in the heterogeneous domain. Respectively, the number of space discretization points per wave length is approximately 15 for $x_1 \notin [-3/20, 3/20]$ in the heterogeneous domain. The mesh is refined every time the angular frequency is doubled, as in the previous test measuring the influence of the pollution error. An example of a solution, computed by the shifted-Laplacian method with $r = 1$, at angular

frequency $\omega = 48\pi$ is plotted in Figure 5.

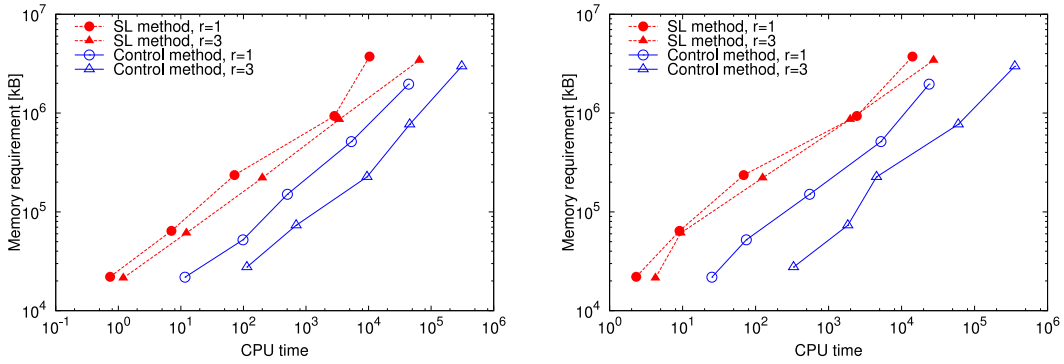

(a) Homogeneous. (b) Heterogeneous.

Figure 3. Memory usage with respect to CPU time (in seconds). On each line, there are points for angular frequencies $\omega = 12\pi, 24\pi, 48\pi, 96\pi, 192\pi$ when ωh is a constant giving approximately 10 discretization points per wavelength.

The CPU times and maximum memory usage for these scattering tests are shown in Figure 3. It can be seen that memory requirement is almost equal between the methods when the frequency is low. As the frequency increases, the GMRES iterations increase in the shifted-Laplacian method. At the same time, the memory needed for storing the Krylov subspace grows as well. The memory requirement of the control method stays constant regardless of the growing of number of iterations. Replacing GMRES method with another method, such as BICGSTAB, would remove this linearly growing memory requirement.

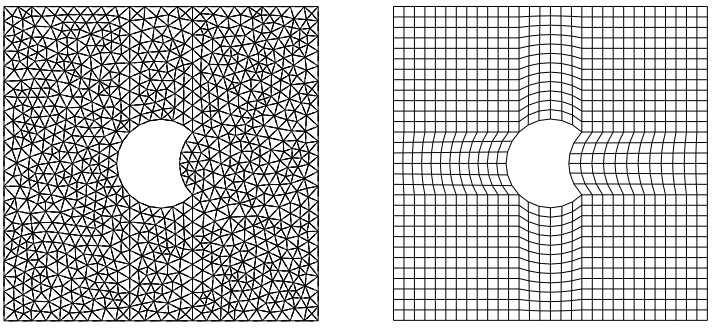

(a) Mesh for the method with shifted-Laplacian preconditioning. (b) Mesh for the control method.

Figure 4. Geometry and the coarsest meshes for both methods with $r = 3$ in scattering tests.

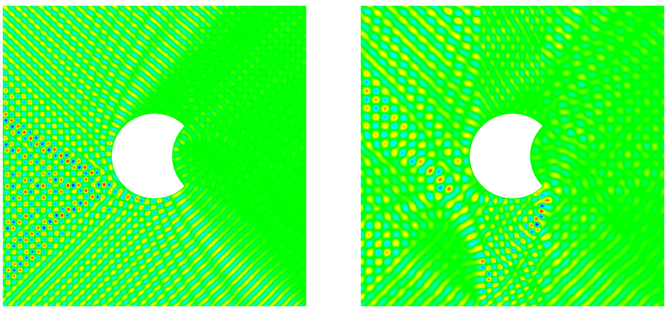

(a) Homogeneous. (b) Heterogeneous.

Figure 5. Solution of the scattering problem in homogeneous and heterogenous domains at angular frequency $\omega = 48\pi$ with the method with shifted-Laplacian preconditioning and $r = 1$.

6 Conclusions

From the numerical tests we can conclude that the control method gave more accurate results but it took more CPU time than the shifted-Laplacian method. One reason for the lower accuracy with the shifted-Laplacian method is the unstructured mesh with changing step size h, as seen in Table 1. It is worth mentioning that the shifted-Laplacian method has quadratic CPU time and linear memory requirement due to the necessity to build Krylov subspace at each GMRES iteration. Choosing some other iterative method, such as BICGSTAB, to the outer iteration could lead to better performance as measured by CPU time. In addition, quadrilateral spectral elements require fewer discretization nodes than triangular finite elements to obtain the same accuracy level.

Acknowledgements

The first author was supported by the Academy of Finland grant #207089. Authors are thankful for Janne Martikainen for letting us use his finite element C++ library in the implementation of the shifted-Laplacian method, and Anssi Pennanen for letting us use his algebraic multigrid code. Jari Toivanen is acknowledged for his advantageous comments on the manuscript. We thank the referees for their comments which helped to improve the paper. Thanks also to our supervisors, Tuomo Rossi and Erkki Heikkola.

References

[1] F. Ihlenburg, Finite Element Analysis of Acoustic Scattering, Springer-Verlag, Berlin, 1998.

[2] I. M. Babuška, S. A. Sauter, Is the pollution effect of the FEM avoidable for the Helmholtz equation considering high wave numbers?, SIAM Journal on numerical analysis 34 (6) (1997) 2392–2423.

[3] G. Cohen, Higher-Order Numerical Methods for Transient Wave Equations, Springer-Verlag, Berlin, 2001.

[4] P. Šolín, K. Segeth, I. Doležel, Higher-Order Finite Element Methods, Chapman & Hall/ CRC Press, Boca Raton, 2004.

[5] L. L. Thompson, A review of finite-element methods for time-harmonic acoustics, Journal of the Acoustical Society of America 119 (3) (2006) 1315–1330.

[6] D. Pathria, G. E. Karniadakis, Spectral element methods for elliptic problems in nonsmooth domains, Journal of Computational Physics 122 (1) (1995) 83–95.

[7] O. Z. Mehdizadeh, M. Paraschivoiu, Investigation of a two-dimensional spectral element method for Helmholtz's equation, Journal of Computational Physics 189 (2003) 111–129.

[8] Y. Saad, Iterative Methods for Sparse Linear Systems, 2nd edition, SIAM, Philadelphia, 2003.

[9] Y. A. Erlangga, C. W. Oosterlee, C. Vuik, A novel multigrid based preconditioner for heterogeneous Helmholtz problems, SIAM Journal on Scientific Computing 27 (4) (2006) 1471–1492.

[10] M. O. Bristeau, R. Glowinski, J. Périaux, Using exact controllability to solve the Helmholtz equation at high wave numbers, in: R. Kleinman, T. Angell, D. Colton, F. Santosa, I. Stakgold (Eds.), Mathematical and Numerical Aspects of Wave Propagation, SIAM, Philadelphia, Pennsylvania, 1993, pp. 113–127.

[11] M. O. Bristeau, R. Glowinski, J. Périaux, Controllability methods for the computation of time-periodic solutions; application to scattering, Journal of Computational Physics 147 (2) (1998) 265–292.

[12] E. Heikkola, S. Mönkölä, A. Pennanen, T. Rossi, Controllability method for acoustic scattering with spectral elements, Journal of Computational and Applied Mathematics 204 (2) (2007) 344–355.

[13] E. Heikkola, S. Mönkölä, A. Pennanen, T. Rossi, Controllability method for the Helmholtz equation with higher-order discretizations, Journal of Computational Physics 225 (2) (2007) 1553–1576.

[14] B. Engquist, A. Majda, Absorbing boundary conditions for numerical simulation of waves, Mathematics of Computation 31 (1977) 629–651.

[15] T. Airaksinen, E. Heikkola, A. Pennanen, J. Toivanen, An algebraic multigrid based shifted-Laplacian preconditioner for the Helmholtz equation, Journal of Computational Physics 226 (2007) 1196–1210.

[16] Y. A. Erlangga, C. Vuik, C. W. Oosterlee, On a class of preconditioners for solving the Helmholtz equation, Applied Numerical Mathematics 50 (3-4) (2004) 409–425.

[17] J. Martikainen, A. Pennanen, T. Rossi, Application of an algebraic multigrid method to incompressible flow problems, Reports of the Department of Mathematical Information Technology, Series B. Scientific Computing, B 2/2006, University of Jyväskylä (2006).

[18] W. Hackbusch, Multigrid Methods and Applications, Springer-Verlag, Berlin, Germany, 1985.